Carbon dioxide electron cooling rates in the atmospheres of Mars and Venus

L. Campbell,[1] M. J. Brunger,[1] and T. N. Rescigno[2]

Received 5 February 2008; revised 14 April 2008; accepted 5 May 2008; published 8 August 2008.

[1] The cooling of electrons in collisions with carbon dioxide in the atmospheres of Venus and Mars is investigated. Calculations are performed with both previously accepted electron energy transfer rates and with new ones determined using more recent theoretical and experimental cross sections for electron impact on CO_2. Emulation of a previous model for Venus confirms the validity of the current model and shows that use of the updated cross sections leads to cooling rates that are lower by one third. Application of the same model to the atmosphere of Mars gives more than double the previous cooling rates at altitudes where the electron temperature is very low.

Citation: Campbell, L., M. J. Brunger, and T. N. Rescigno (2008), Carbon dioxide electron cooling rates in the atmospheres of Mars and Venus, *J. Geophys. Res.*, *113*, E08008, doi:10.1029/2008JE003099.

1. Introduction

[2] Free electrons in planetary atmospheres collide with molecules, producing vibrational excitation. The excitation energy can then be lost by radiative decay, with the emitted infrared radiation removing energy from the atmosphere.

[3] Electron cooling by electron impact excitation of carbon dioxide was identified [*Morrison and Greene*, 1978] as an important energy transfer process in the Martian atmosphere, and probably important for Venus. *Morrison and Greene* [1978] calculated electron energy loss rates, elsewhere named electron energy transfer rates [*Pavlov*, 1998], these being the rates of energy loss per unit electron and molecule density. These loss rates were calculated as a function of electron temperature and have been used as a parameter in modeling of the ionosphere of Venus [*Strangeway*, 1996].

[4] In the past few years new measurements and theoretical calculations of electron impact on CO_2 have been made. There are also much more data characterizing the atmospheres of Mars and Venus than were available in 1978. Hence it is timely to repeat the calculations of *Morrison and Greene* [1978] and consider the implications for modeling of energy transfer in the atmospheres of Mars and Venus.

[5] In this work the recent experimental and theoretical cross sections for electron impact excitation of 7 vibrational modes of CO_2 are considered and an optimum set is assembled. The electron energy transfer rates are calculated for this set and compared with those predicted by *Morrison and Greene* [1978]. The available measurements of the relevant atmospheric parameters of Mars and Venus are considered and particular sets chosen. The electron cooling rates (for excitation from the ground level of CO_2) are calculated for Venus and compared with those of a previous model, verifying the method of calculation. It is found that the cooling rates are lower ($\sim$33%) when the updated cross section set is used. The same procedure applied for the atmosphere of Mars shows that, at altitudes where the electron temperature is very low, the cooling rates are substantially greater when the updated cross section set is used. This may provide an explanation as to why models of the Martian atmosphere overestimate the neutral temperature in the altitude range 100–130 km.

2. Electron Impact Cross Sections

[6] The initial calculations of CO_2 electron energy loss rates [*Morrison and Greene*, 1978] were based on integral cross sections deduced from swarm measurements. In the current work we have assembled a set of integral cross sections based on crossed-beam measurements and recent theoretical calculations.

2.1. Measured Cross Sections

[7] A recommended set of integral cross sections (ICSs) for electron impact excitation of the (000), (010), (100) and (001) modes in carbon dioxide was presented in a review of earlier measurements [*Brunger et al.*, 2003]. Differential cross sections (DCSs) for electron impact excitation of the (010), (100), (001) and (020) vibrational modes were measured in a crossed-beam experiment for 1.5–30-eV electrons [*Kitajima et al.*, 2001]. The energy dependence of the absolute DCSs (at scattering angle 135°) for the Fermi dyad [(100), (020)] [*Allan*, 2001] and the (000), (001) and (101) modes [*Allan*, 2002] and relative DCSs (at 90°) for the Fermi triad [(200) + (120) + (040)] [*Allan*, 2002] was measured with an electron spectrometer that allows the threshold peaks at low electron energies to be seen.

2.2. Theoretical Cross Sections

[8] In a fully *ab initio* study, *McCurdy et al.* [2003] used the complex Kohn variational method to predict ICSs for

[1] ARC Center for Antimatter-Matter Studies, Flinders University, South Australia, Australia.
[2] Chemical Sciences, Lawrence Berkeley National Laboratory, Berkeley, California, USA.

0148-0227/08/2008JE003099

Table 1. Algorithms for Combination of Cross Sections in Various Energy Ranges[a]

	Impact energy (eV)					
Mode	<0.3	0.3–0.5	0.5–2.0	2.0–3.0	3.0–4.7	>4.7
(000)		Allan	*max*[Allan, Brunger]		Brunger	
(100)		Allan		*max*[Allan, DK + Brunger(10 eV)]		
(020)			*min*[McCurdy, DK]		McCurdy	*max*[McCurdy, DK]
(200)			*max*[Allan (scaled to McCurdy at 2.0 eV), McCurdy]			
(120)				McCurdy		
(040)				McCurdy		
(001)	Allan			*max*[Allan, DK]		
(010)		Allan		*max*[Allan, DK + Brunger(3.6, 10, 20 eV)]		

[a]"DK" represents current ICSs derived from measured DCSs of *Kitajima et al.* [2001], and "+ Brunger(*list* eV)" indicates addition of the ICSs at the energies in *list* from the review [*Brunger et al.*, 2003]. Underlining indicates linear interpolation to or extrapolation from the discrete values. min[] and max[] represent the minimum and maximum of the ICSs from the sources in brackets. "Allan" represents excitation functions of *Allan* [2002] scaled by 4π and "McCurdy" the theoretical ICSs of *McCurdy et al.* [2003].

electron-impact excitation of the components of the Fermi dyad [modes (100) and (020)] and of the Fermi triad [(200), (120) and (040)] in CO_2.

2.3. Cross-Section Database

[9] We have combined the measured and calculated cross sections to produce an optimum set of integral cross sections for the calculations that follow. A phase-shift analysis [*Campbell et al.*, 2001] was used to determine the ICSs from the measured DCSs of *Kitajima et al.* [2001]. These ICSs are supplemented with values at some energies from the set of *Brunger et al.* [2003]. The excitation functions of Allan were scaled by 4π, except for the (200) mode as noted below, to produce estimated ICSs. Values from these various sources were combined as also explained below for each vibrational mode. The algorithms implementing the combination are given in Table 1 and the resulting "optimum" set of ICSs is shown in Figure 1. Also shown in Figure 1 are the cross sections of *Bulos and Phelps* [1976] which were used in the earlier calculations [*Morrison and Greene*, 1978] of electron energy loss rates.

2.3.1. (000)

[10] The ICSs for elastic collisions are presented for completeness. They do not lead to energy loss via subsequent radiative decay and have a much smaller cooling effect than vibrational excitation [*Strangeway*, 1996], so they are not included in the calculations to follow. The values of *Brunger et al.* [2003] are used, except for the threshold peak where the scaled values of Allan are employed.

2.3.2. (100)

[11] The current ICSs derived from the DCSs of *Kitajima et al.* [2001] plus the 10-eV ICS of *Brunger et al.* [2003] are used, except for the threshold peak and the peak around 3.5 eV, where the FR_{II} component of the Fermi dyad measured by Allan is employed.

2.3.3. (020)

[12] For the peak around 4 eV the ICSs of *McCurdy et al.* [2003] are preferred, while the ICSs derived from the DCSs of *Kitajima et al.* [2001] are used for lower and higher energies. At lower energies the ICS of *McCurdy et al.* [2003] rises with decreasing energy in a way that is not supported by the measurements, and at higher energies the theoretical values are zero while the measured values are non-zero. Under these circumstances the measured values are used in these cases.

2.3.4. (200)

[13] The threshold peak of Allan is added to the predictions of *McCurdy et al.* [2003], with the values of Allan scaled to match the ICS of *McCurdy et al.* [2003] at 2 eV.

2.3.5. (120), (040)

[14] The calculated values of *McCurdy et al.* [2003] are used.

2.3.6. (001)

[15] The ICSs derived from the DCSs of *Kitajima et al.* [2001] are combined with the threshold peak measured by Allan.

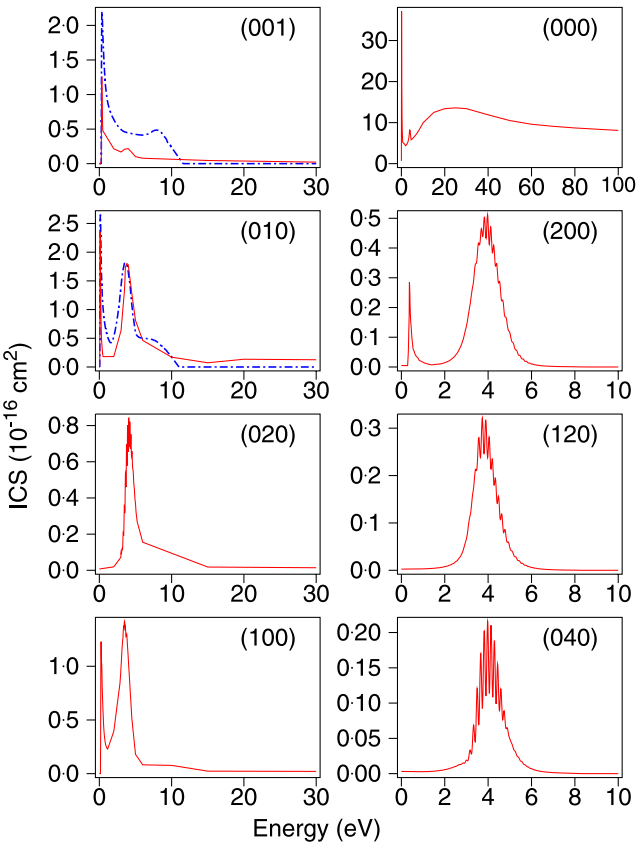

Figure 1. Integral cross sections for electron impact on CO_2 as a function of electron energy for elastic collisions (000) and seven vibrational modes (as labeled), in the updated set (—) and earlier swarm measurements [*Bulos and Phelps*, 1976] (-·-).

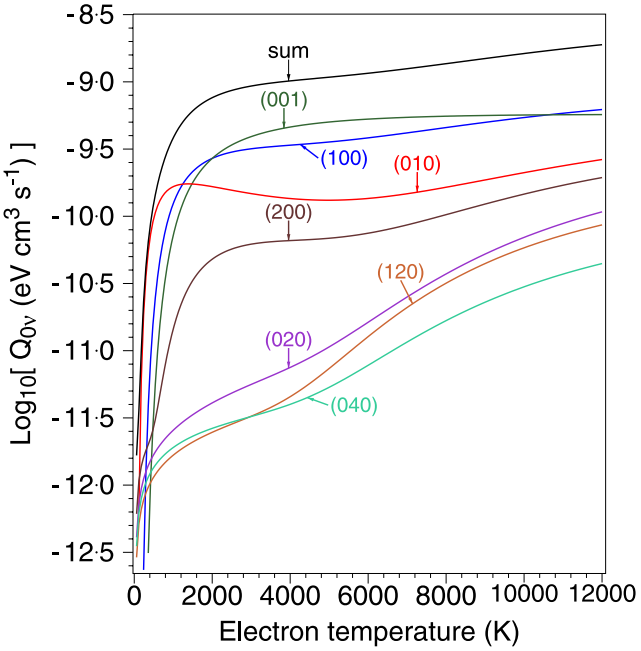

Figure 2. Calculated electron energy transfer rates for the seven vibrational modes and for their sum, as a function of electron temperature.

2.3.7. (010)

[16] The ICSs derived from the DCSs of *Kitajima et al.* [2001] are combined with the ICSs at 3.6, 10 and 20 eV of *Brunger et al.* [2003] and with the threshold peak of Allan.

3. Electron Energy Transfer Rates

[17] The electron energy transfer rates $Q_{0\nu}$ are calculated as a function of electron temperature T_e using the formulation of *Pavlov* [1998]:

$$Q_{0\nu} = E_\nu \left\{ 8kT_e(\pi m_e)^{-1} \right\}^{0.5} \int_0^\infty \sigma_{0\nu}(x) x \exp(-x) dx \qquad (1)$$

where $x = E(kT_e)^{-1}$, E is the electron energy, E_ν is the energy of mode ν, $\sigma_{0\nu}$ is the ICS for excitation from the ground level to mode ν, k is Boltzmann's constant and m_e is the mass of the electron.

[18] Electron energy transfer rates for the seven vibrational modes listed in section 2, calculated using equation (1), are plotted as a function of T_e in Figure 2, along with the sum for the seven modes. At low temperatures the main contributions to the energy transfer rates are for the modes (001), (100), (010) and (200), which is expected as these have threshold peaks which are excited by the low-energy electrons which predominate at low temperatures.

[19] These rates are compared with those of the previous calculations [*Morrison and Greene*, 1978] in Figure 3. The individual components of the Fermi dyad and triad were not available to *Morrison and Greene* [1978], so to make a comparison the current ICSs for each of the dyad and triad have been combined. The differences between the current and the previous rates are:

[20] 1. at higher temperatures, the rates using the current ICSs are substantially smaller for the (010) and (001) modes and for the dyad;

[21] 2. at temperatures below 4000 K, the rates using the current ICSs are substantially larger for the Fermi triad;

[22] 3. at low temperatures, the current rates are higher for all modes, although the difference is not as great for the (001) mode;

[23] 4. the sum of the current rates is higher at the low temperatures (<600 K) and lower for higher temperatures.

4. Atmospheric Parameters

[24] To calculate electron cooling by excitation from the ground state of carbon dioxide in an atmosphere, the required parameters are the electron temperature and density and the density of carbon dioxide. Optimum sets of these parameters were drawn together in this work from the available measurements, with some theoretical values used where measurements are not available. Since the publication of *Morrison and Greene* [1978], there has been further analysis of the 1976 Viking observations of the atmosphere of Mars, as well as new observations of both Venus and Mars by orbiting spacecraft.

[25] We assume a Maxwellian distribution of thermal electrons for consistency with the calculations of *Morrison and Greene* [1978]. This assumption is consistent with measurements for the Martian atmosphere: *Hanson and*

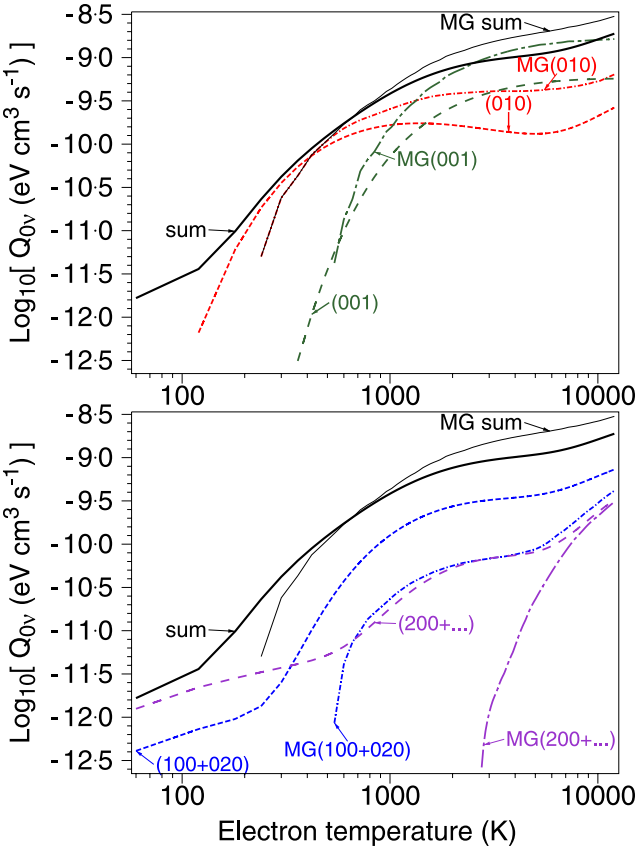

Figure 3. Comparison of present electron energy transfer rates (as labeled) with previous calculations [*Morrison and Greene*, 1978] (as labeled with prefix "MG"). Note that "(200 + . . .)" represents "(200 + 120 + 040)" and that the "sum" in both panels is the sum for all 7 modes.

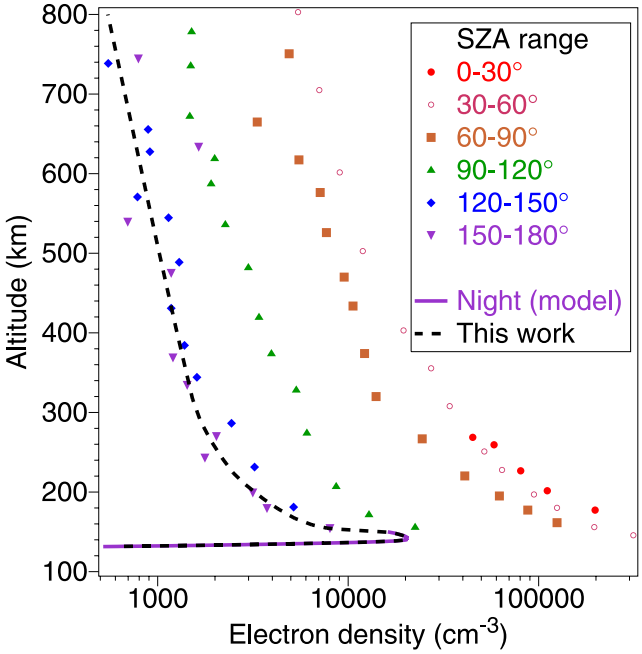

Figure 4. Measurements of electron density in the atmosphere of Venus for various ranges of solar zenith angle (SZA), *Strangeway*'s [1996] nighttime model (—) and the current fit to the nighttime values (- - -).

Mantas [1988] presented evidence that most of the free electrons are in a Maxwellian thermal distribution.

4.1. Atmospheric Parameters for Venus

[26] Densities of CO_2 in the atmosphere of Venus were measured by Pioneer Venus in 1978–1980 and again, over a larger height range, during its re-entry phase in 1992 [*Kasprzak et al.*, 1993]. *Kasprzak et al.* [1993] fit predictions of a model called "VTS3" to the measurements, and we use these fitted values in the calculations that follow.

[27] Measurements of the electron density and temperature were made by Pioneer Venus in 1978 [*Miller et al.*, 1980]. These do not cover the altitude range 100–150 km of the previous calculations [*Strangeway*, 1996] of electron cooling rates, so the values of electron density and temperature calculated in the model of *Strangeway* [1996] are used here. The measurements and the calculated nighttime values of Strangeway for electron density and temperature are shown in Figures 4 and 5, respectively, together with functions fitted to the combination that are used in the current work. The figures show that the calculated values of Strangeway and the measurements at night (i.e., solar zenith angle = 150°–180°) are not inconsistent, in that a function with a reasonable shape can fit to both.

4.2. Atmospheric Parameters for Mars

[28] Electron densities and temperatures and densities of CO_2 in the atmosphere of Mars were measured *in situ* by the Viking landers during descent in 1976. As the electron data for Viking 2 were unsatisfactory [*Hanson and Mantas*, 1988], the current calculations neglect the Viking 2 measurements for CO_2 density and only use data from Viking 1, to have a consistent set of measurements.

[29] The CO_2 densities used here are from a fit [*Nier and McElroy*, 1977] to the Viking 1 data:

$$[CO_2] = 10.0^{15.930-0.042696z} \quad (2)$$

where $[CO_2]$ is the density (cm^{-3}) of CO_2 at height z (km).

[30] The Viking 1 measurements of electron density [*Hanson and Mantas*, 1988] are shown in Figure 6 for the altitude range 138–393 km. More recently profiles of electron densities have been measured remotely by the Mars Global Surveyor [*Martinis et al.*, 2003] for 100–200 km. The maximum and minimum values are shown in Figure 6. In the current work a fit to all these measurements is made, shown by the solid line in Figure 6.

[31] Electron temperatures deduced by Hanson and Mantas from the Viking 1 data are plotted in Figure 7 for the altitude range 207–329 km. In the absence of measurements at lower altitudes, we use a calculated electron temperature profile [*Choi et al.*, 1998] that best matches the Viking measurements. Figure 6 also includes measurements and calculations of the neutral temperature, which will be referred to in later discussion.

5. Electron Cooling Rates

[32] The electron cooling rate L due to electron impact excitation of ground-state CO_2 in an atmosphere is calculated here as

$$L = N_e[CO_2(0)]\sum_{\nu=1}^{7} Q_{0\nu} \quad (3)$$

where N_e is the electron density, $[CO_2(0)]$ is the ground-state CO_2 density and $\nu = 1$–7 represents the 7 vibrational

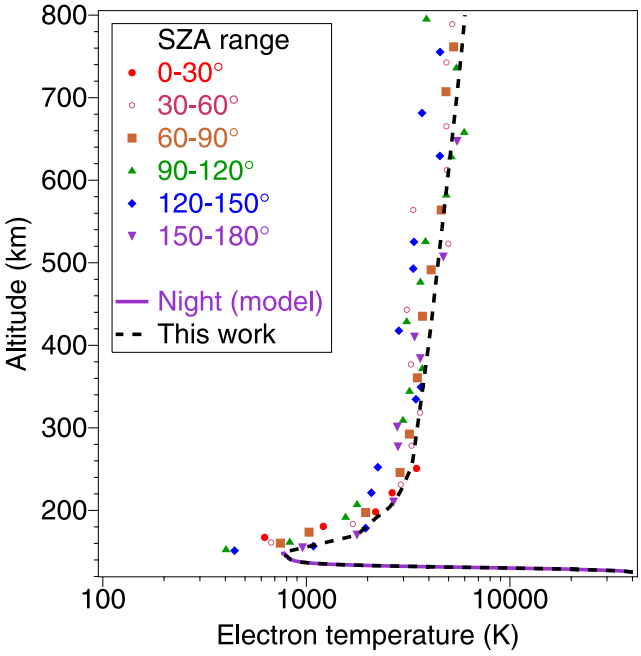

Figure 5. Measurements of electron temperature in the atmosphere of Venus for various ranges of solar zenith angle (SZA), *Strangeway*'s [1996] nighttime model (—) and the current fit to the nighttime values (- - -).

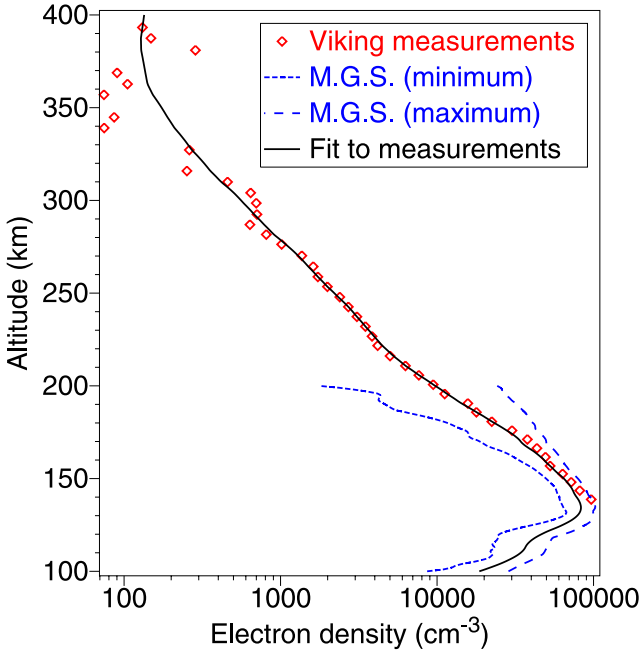

Figure 6. Measurements of electron density in the atmosphere of Mars for Viking 1 observations (◇), the maximum (– – –) and minimum (- - -) values measured by the Mars Global Surveyor, and the fit (—) used in the current model.

modes outlined above. Electron cooling rates in the atmosphere of Venus were calculated previously [*Strangeway*, 1996] using the electron energy loss rates given by *Morrison and Greene* [1978]. *Strangeway*'s [1996] calculations are emulated here to verify the current model, then repeated using the new cross sections. The same model is then applied for the atmosphere of Mars.

5.1. Cooling Rates for Venus

[33] *Strangeway* [1996] calculated the cooling rates due to vibrational excitation of CO_2 for a "typical nightside ionosphere". These [from *Strangeway*, 1996, Figure 6] are labeled as "Strangeway graph" in Figure 8. Evaluation of a formula [*Strangeway*, 1996, equation (A3)] for the ionospheric parameters quoted for Strangeway's figure 6 gives the results labeled as "Strangeway formula" in Figure 8. As both the ionospheric parameters and the "Strangeway graph" are digitized from graphs with logarithmic scales, the discrepancies between the graph and the formula may be due to the cumulative effects of digitization errors.

[34] The ionospheric parameters from *Strangeway* [1996, Figure 6] and the electron energy loss rates of *Morrison and Greene* [1978] are used in the current model, giving the cooling rates labeled "Morrison and Greene" in Figure 8. These values are close to those of Strangeway's formula for altitudes above 131 km, and very close to Strangeway's curve in figure 6 below 129 km. This does not lead to an explanation for the discrepancies between Strangeway's graph and formula, but it does verify the current method of calculating the cooling rates, in as much as the current results are close to one case or the other in the results of Strangeway.

[35] The current model is now applied using the electron energy transfer rates determined from the new cross section set, giving the cooling rates labeled "New cross sections"

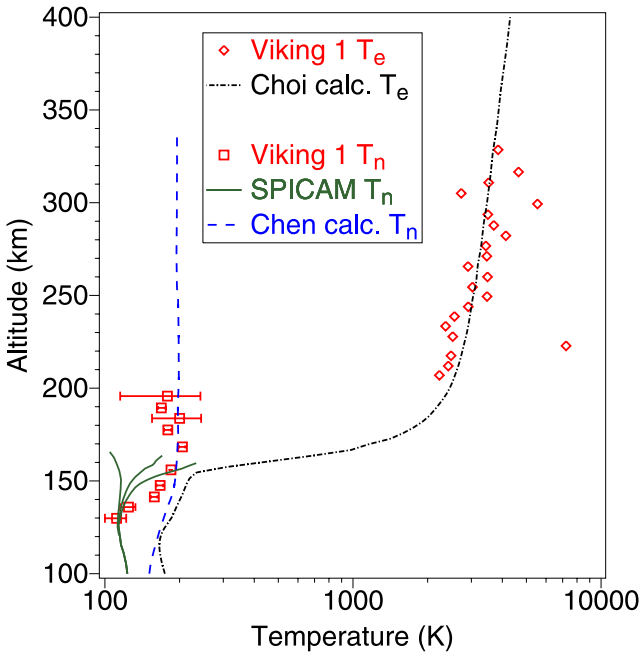

Figure 7. For Mars, measurements of electron (◇) and neutral (□) temperatures by Viking 1, measurements of neutral temperatures made by Mars Express (—), electron temperatures calculated by *Choi et al.* [1998] (- · - · -), and neutral temperatures calculated by *Chen et al.* [1978] (- -).

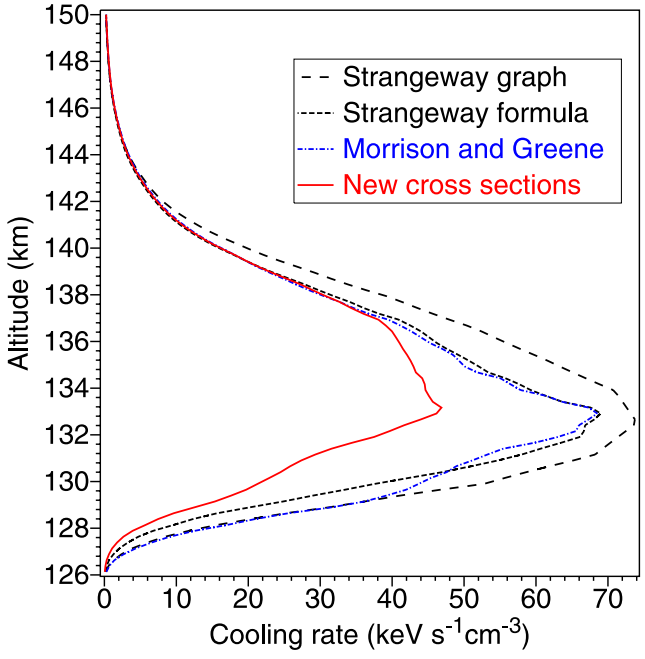

Figure 8. Electron cooling rates as a function of altitude in the atmosphere of Venus, presented by *Strangeway* [1996] (– – –), calculated using a formula of Strangeway (- - -), calculated by the current model using the loss rates of *Morrison and Greene* [1978] (- · - · -), and calculated by the current model using the updated ICSs (—).

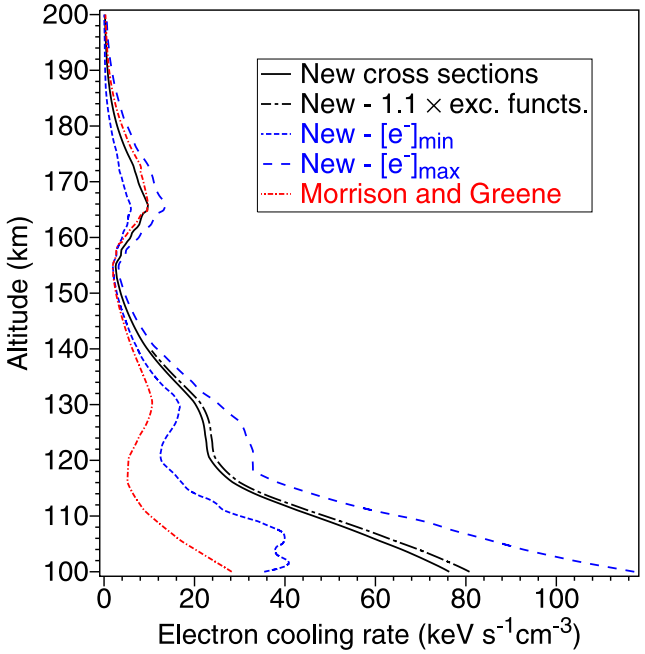

Figure 9. Electron cooling rates as a function of altitude in the atmosphere of Mars, calculated using the electron energy loss rates of *Morrison and Greene* [1978] (- · - ·-), and using the updated cross sections with the fitted electron density (—), with the maximum (– – –) and minimum (- - -) electron densities measured by the Mars Global Surveyor, and with the fitted electron density with an increase of 10% in the 4π-scaled excitation functions (— · —).

in Figure 8. These are lower (by one third) than those calculated using the rates of *Morrison and Greene* [1978].

5.2. Cooling Rates for Mars

[36] In Figure 9, the electron cooling rates for the atmosphere of Mars are shown, calculated using the loss rates of *Morrison and Greene* [1978] and using the new cross section set. Below ∼140 km the cooling rates calculated with the new cross sections are substantially larger than those based on the rates of *Morrison and Greene* [1978], reaching a factor of almost 3 times larger at 100 km.

[37] The calculations with the new cross sections are repeated for the minimum and maximum observed electron densities [*Martinis et al.*, 2003]. For the minimum electron densities, the cooling rates are still substantially larger than those using the previous loss rates. Hence the effect of using the new cross section set leads to an increase in the calculated cooling rate which is greater than is involved in the day-to-day variation in the electron density.

[38] The uncertainty due to using the scaled excitation functions of *Allan* [2001, 2002] for the (100), (001) and (010) modes is investigated by increasing their values by 10%. (As the scaled functions were measured at 135°, while the cross section is expected to be larger at forward angles, it is possible that the 4π-scaled values are underestimated.) The 10% increase produces an ∼6% increase in the cooling rate at low altitudes, indicating that the contribution of the three modes is a substantial fraction of the total at low electron temperatures. Hence it is desirable that ICSs be measured for the three modes at low electron energies, although these would be expected only to enhance the large increase in cooling rates that we predict with the new cross sections.

[39] This substantially greater electron cooling rate may explain why observed neutral temperatures in the atmosphere of Mars below 130 km are less than predicted in modeling. In Figure 7, the measurements by Viking 1 [*Nier and McElroy*, 1977] show neutral temperatures well below those predicted in a model [*Chen et al.*, 1978]. Also shown are more recent temperature measurements by the SPICAM UV spectrometer aboard Mars Express [*Forget et al.*, 2007]. (These temperatures were presented as a function of pressure and have been converted to a function of height here by assuming a scale height of 11 km.) The SPICAM temperatures are consistent with the lowest Viking values and, in the altitude range 90–140 km, are significantly less than predicted in modeling for the conditions of the measurements [*Forget et al.*, 2007].

[40] As part of the energy in vibrationally excited CO_2 will be emitted as infrared radiation and thus lost from the atmosphere, a larger electron cooling rate should lead to a lower overall temperature. Thus the higher electron energy transfer rates found in this work may provide the extra cooling component that is required to account for the unexpectedly low neutral temperatures in the 100–130-km region of the atmosphere of Mars.

6. Conclusions

[41] A set of integral cross sections for electron impact vibrational excitation of CO_2 is presented and corresponding electron energy transfer rates are calculated. These rates differ from previous ones, in that they give lower rates at higher electron temperatures and higher rates at low temperatures. The effect of using the updated rates is investigated for electron cooling in the atmospheres of Mars and Venus. Emulation of previous calculations for Venus confirms the validity of the current model. For Venus, application of the updated transfer rates leads to a reduction of at least 30% in the electron cooling. Applying the updated transfer rates to the altitudes where the electron temperatures are very low in the atmosphere of Mars, gives cooling rates that are substantially larger (by a factor of 2–3) than given by using the earlier transfer rates. It is suggested that inclusion of the updated electron energy transfer rates in Martian atmospheric models may enable them to predict the very low neutral temperatures that are seen in observations at these altitudes.

[42] **Acknowledgments.** This work was supported by the Australian Research Council and Flinders University. TNR was supported by the USDOE, OBES Division of Chemical Sciences.

References

Allan, M. (2001), Selectivity in the excitation of the Fermi-coupled vibrations in CO_2 by impact of slow electrons, *Phys. Rev. Lett.*, *87*, 033201, doi:10.1103/PhysRevLett.87.0332010-1-19.

Allan, M. (2002), Vibrational structures in electron–CO_2 scattering below the $^2\Pi_u$ shape resonance, *J. Phys. B: At., Mol. Opt. Phys.*, *35*, L387–L395.

Brunger, M. J., S. J. Buckman, and M. T. Elford (2003), Excitation cross sections, in *Photon and Electron Interactions with Atoms, Molecules and*

Ions, Landolt-Börnstein vol. I/17C, edited by Y. Itikawa, pp. 6-180–6-181, chap. 6.4, Springer, New York.

Bulos, B. R., and A. V. Phelps (1976), Excitation of the 4.3-μm bands of CO_2 by low-energy electrons, *Phys. Rev. A*, *14*, 615–629.

Campbell, L., M. J. Brunger, A. M. Nolan, L. J. Kelly, A. B. Wedding, J. Harrison, P. J. O. Teubner, D. C. Cartwright, and B. McLaughlin (2001), Integral cross sections for electron impact excitation of electronic states of N_2, *J. Phys. B: At., Mol. Opt. Phys.*, *34*, 1185–1199.

Chen, R. H., T. E. Cravens, and A. F. Nagy (1978), The Martian ionosphere in light of the Viking observations, *J. Geophys. Res.*, *83*, 3871–3876.

Choi, Y. W., J. Kim, K. W. Min, A. F. Nagy, and K. I. Oyama (1998), Effect of the magnetic field on the energetics of Mars ionosphere, *Geophys. Res. Lett.*, *25*, 2753–2756.

Forget, F., J. L. Bertaux, F. Montmessin, E. Quemerais, F. González-Galindo, S. Lebonnois, E. Dimarellis, A. Reberac, and M. A. López-Valverde (2007), The density and temperatures of the upper Martian atmosphere measured by stellar occultations with Mars Express SPICAM, in *European Mars Science and Exploration Conference: Mars Express & ExoMars, ESTEC, Netherlands, 12–16 November, 2007*. (Available at http://www.rssd.esa.int/sys/include/pubs_display.php?project=MarsEXPRESS&id=2778526)

Hanson, W. B., and G. P. Mantas (1988), Viking electron temperature measurements: Evidence for a magnetic field in the Martian ionosphere, *J. Geophys. Res.*, *93*, 7538–7544.

Kasprzak, W. T., H. B. Niemann, A. E. Hedin, S. W. Bougher, and D. M. Hunten (1993), Neutral composition measurements by the Pioneer Venus neutral mass spectrometer during orbiter re-entry, *Geophys. Res. Lett.*, *20*, 2747–2750.

Kitajima, M., S. Watanabe, H. Tanaka, M. Takekawa, M. Kimura, and Y. Itikawa (2001), Differential cross sections for vibrational excitation of CO_2 by 1.5–30 eV electrons, *J. Phys. B*, *34*, 1929–1940.

Martinis, C. R., J. K. Wilson, and M. J. Mendillo (2003), Modeling day-to-day ionospheric variability on Mars, *J. Geophys. Res.*, *108*(A10), 1383, doi:10.1029/2003JA009973.

McCurdy, C. W., W. A. Isaacs, H.-D. Meyer, and T. N. Rescigno (2003), Resonant vibrational excitation of CO_2 by electron impact: Nuclear dynamics on the coupled components of the $^2\Pi_u$ resonance, *Phys. Rev. A*, *67*, 042708, doi:10.1103/PhysRevA.67.042708-1-19.

Miller, K. L., W. C. Knudsen, K. Spenner, R. C. Whitten, and V. Novak (1980), Solar zenith angle dependence of ionospheric ion and electron temperatures and density on Venus, *J. Geophys. Res.*, *85*, 7759–7764.

Morrison, M. A., and A. E. Greene (1978), Electron cooling by excitation of carbon dioxide, *J. Geophys. Res.*, *83*, 1172–1174.

Nier, A. O., and M. B. McElroy (1977), Composition and structure of Mars' upper atmosphere: Results from the neutral mass spectrometers on Viking 1 and 2, *J. Geophys. Res.*, *82*, 4341–4349.

Pavlov, A. V. (1998), New electron energy transfer and cooling rates by excitation of O_2, *Ann. Geophys.*, *16*, 1007–1013.

Strangeway, R. J. (1996), Collisional Joule dissipation in the ionosphere of Venus: The importance of electron heat conduction, *J. Geophys. Res.*, *101*, 2279–2295.

M. J. Brunger and L. Campbell, ARC Centre for Antimatter-Matter Studies, School of Chemistry, Physics and Earth Sciences, Flinders University, GPO Box 2100, Adelaide, SA 5001, Australia. (laurence.campbell@flinders.edu.au)

T. N. Rescigno, Chemical Sciences, Lawrence Berkeley National Laboratory, 1 Cyclotron Road, Mail Stop 2R0100, Berkeley, CA 94720-8196, USA.